Observatório Nacional

Programa de Pós-Graduação em Geofísica

Dissertação de mestrado

A MEAN-FIELD BABCOCK-LEIGHTON SOLAR DYNAMO MODEL WITH LONG-TERM VARIABILITY

Sabrina Maite Sanchez

Orientadora:
Katia Jasbinschek dos Reis Pinheiro

Co-orientador:
Alexandre Fournier

Rio de Janeiro
2012

"A MEAN-FIELD BABCOCK-LEIGHTON SOLAR DYNAMO MODEL WITH LONG TERM VARIABILITY"

SABRINA MAITE SANCHEZ

DISSERTAÇÃO SUBMETIDA AO CORPO DOCENTE DO PROGRAMA DE PÓS-GRADUAÇÃO EM GEOFÍSICA DO OBSERVATÓRIO NACIONAL COMO PARTE DOS REQUISITOS NECESSÁRIOS PARA A OBTENÇÃO DO GRAU DE MESTRE EM GEOFÍSICA.

Aprovada por:

Dra. Kátia Jasbinschek dos Reis Pinheiro – ON/MCTI
(orientadora)

Dr. Ricardo Ivan Ferreira da Trindade – IAG/USP

Oscar Toshiaki Matsuura – IAG/USP

RIO DE JANEIRO – BRASIL

31 DE AGOSTO DE 2012

A MEAN-FIELD BABCOCK-LEIGHTON SOLAR DYNAMO MODEL WITH LONG-TERM VARIABILITY

Sabrina Maite Sanchez

TESE SUBMETIDA AO CORPO DOCENTE DO PROGRAMA DE PÓS-GRADUAÇÃO EM GEOFíSICA DO OBSERVATÓRIO NACIONAL COMO PARTE DOS REQUISITOS NECESSÁRIOS PARA A OBTENÇÃO DO GRAU DE MESTRE EM GEOFíSICA.

Aprovada por:

Dra. Katia Jasbinschek dos Reis Pinheiro (orientadora)

Dr. Oscar Toshiaki Matsuura

Dr. Ricardo Ivan Ferreira da Trindade

Dr. Andrés Reinaldo Rodriguez Papa (suplente)

Dr. Cosme Ferreira da Ponte Neto (suplente)

RIO DE JANEIRO- BRASIL- 2012

Contents

1 Resumo **2**

2 Abstract **3**

3 Introduction **4**

4 Model formulation **7**

5 Mathematical description **11**

6 Numerical simulation **15**

7 Results **16**

8 Conclusion **20**

9 Acknowledgements **21**

10 Appendix **22**

11 References **24**

1 Resumo

Modelos do dínamo solar baseados no mecanismo de Babcock-Leighton obtiveram sucesso em reproduzir algumas das principais características da dinâmica do campo magnético do Sol. No entanto, considerando que tal mecanismo opera somente a partir de um limite mínimo do campo magnético, ele não provê um processo apropriado de regeneração do campo que caracterize um dínamo auto-sustentável. Neste trabalho consideramos a existência de um efeito α concomitante com o cenário disposto pelo modelo de Babcock-Leighton em uma simulação numérica 2D de campo médio. Diferentes fatores de limitação de intensidade do campo foram usados para os dois processos de regeneração do campo poloidal. Excetuando-se o critério da anti-paridade do campo magnético, as principais características do campo magnético solar foram reproduzidas: reversão cíclica, migração ao equador dos intensos campos toroidais em médias latitudes, deslocamento aos pólos do campo magnético polar na superfície, e a relação de anti-fase entre ambos. A variabilidade de longo período resultou em alguns casos na existência de épocas duradouras de mínimo de atividade magnética e posterior recuperação , como no Mínimo de Maunder. Tendo como base a observação de uma atividade residual durante os períodos de mínima atividade, sugerimos que tais períodos são causados por uma predominância do efeito α sobre o mecanismo de Babcock-Leighton na regeneração do campo poloidal.

2 Abstract

Dynamo models relying on the Babcock-Leighton mechanism are successful in reproducing most of the solar magnetic field dynamical characteristics. However, considering that such models work only above a lower magnetic field threshold, they do not provide an appropriate magnetic field regeneration process characterizing a self-sustainable dynamo. In this work we consider the existence of an additional α-effect to the Babcock-Leighton scenario in a mean-field 2D numerical model. Both poloidal field regenerating mechanisms were treated with two different strength-limiting factors. Apart from the solar anti-symmetric parity behaviour, the main solar features were reproduced: cyclic reversion, mid-latitudinal equatorward migration of strong toroidal field, poleward migration of polar surface radial fields, and the anti-phase relation between both. Long-term variability of the solutions allowed periods of extended minimum activity and posterior recovery, as the Maunder Minimum. Based on the observation of a residual activity during minima periods, we suggest they are caused by a predominance of the α-effect over the Babcock-Leighton mechanism in regenerating the poloidal field.

3 Introduction

The Sun is a magnetic active star, which undergoes periods of high and low magnetic activity approximately each 11 years. Its dynamical behavior imposes important consequences to the terrestrial environment, not only producing magnetic storms, which affect satellite operation (Baker 2000), but also possibly having an important role in Earth's climate long-term variability (Haigh 2003).

By magnetic activity we understand the appearance of sunspots, characterized by their lower luminosity (in comparison with the overall photosphere) and intense magnetic fields (Solanki 2003). Sunspots usually appear in pairs of opposite polarities roughly aligned with the E-W direction, what evidences they are the surface manifestations of concentrated azimuthal magnetic fields (toroidal flux tubes), arising from the deep of the convection zone by magnetic buoyancy (Parker 1979). It is important to mention that the alignment with the equatorial direction is not perfect: sunspot pairs often display a systematic tilt, the leading spot being nearer the equator than the following one - Joy's law. Sunspots generally appear within a 30^o latitudinal band in each side of the equator, displaying opposite polarity configuration in each hemisphere - Hale's polarity law. As the activity cycle is initiated, sunspot appearance migrates towards the equatorial region, and after the end of the 11 years cycle they begin again to appear at approximately 30^o, but with an opposite polarity configuration. This means the full magnetic sunspot cycle is twice the activity period. Moreover, sunspots cyclic appearance is directly linked with the variability of the large-scale solar magnetic field: during episodes of maximum activity, the polar magnetic field undergoes polarity inversion (Makarov et al. 2000).

All such outstandingly well organized features of the dynamical solar magnetic field are supposed to originate from a natural dynamo process, regenerating the magnetic field against

ohmic dissipation by convective motions of the conducting plasma (Ossendrijver 2003). These features also indicate the large-scale magnetic field is divided into two main components that evolve within a phase lag: the toroidal (azimuthal) magnetic field, associated with sunspots, and the poloidal (meridional) field, represented by the polar field. Despite the regular character evidenced by the solar cycle, it also undergoes amplitude and frequency fluctuations (Hathaway 2010). The most striking examples of this variability are the periods of minimum activity, such as the Maunder Minimum. At such episode, covering the years from 1645 to 1715, sunspots were rarely seen. However, indirect data indicated the persistence, although weak, of the solar cycle (Beer et al. 1998). Much discussion exists on the cause of this peculiar variability, and how the answers could aid in accessing unconstrained properties of the solar dynamo mechanism.

Modeling of the solar dynamo has shed light into some of the main process responsible for the solar cycle (Charbonneau 2010), qualitatively known as the α and ω-effects. The ω-effect symbolizes the shearing action of the differential rotation of the flow on an initial poloidal field, giving rise to a toroidal field. Through the advent of helioseismology, the large-scale flow has been mapped in detail (Schou et al. 1998). The region of strongest angular velocity gradients, and so the preferred site for the ω-effect, was found to be at the base of the convection zone: the tachocline (Howe et al. 2000a). Turbulent motions associated with the Coriolis force, in turn, would twist the toroidal field, generating a new component of the poloidal field and thus maintaining the solar cycle (Parker 1955). This latter process is now known as the mean-field α-effect, and unlike the ω-effect, is far from being totally understood, as well as the preferred place for its action. It is also known that the Lorentz force back-reaction of strong magnetic fields inhibits turbulence; so the conventional α-effect would not lead to great effectiveness in regenerating the poloidal field for a strong magnetic field regime (Cattaneo and Hughes 1996). Other processes, like the ones relying on the Babcock-Leighton mechanism, may have

an important role on the poloidal field regeneration. Differently from the mean α-effect, the Babcock-Leighton mechanism relies on the diffusion of the sunspots magnetic fields, operating at the solar surface (Babcock 1961, Leighton 1969).

Numerical 2D models, relying on the longitudinal symmetry of the solar magnetic field, are widely used as a tool to access the validity of the main effects supposed to drive the solar dynamo. Many of the solar features are well reproduced by numerical models, but no agreement is achieved considering the particular causes. Variability of the solar cycle, for example, is generally explained by either stochastic forcing (Choudhuri 1992, Charbonneau and Dikpati 2000) or dynamical nonlinearities (Bushby 2006). Alternatively, simple form of time-delays arising from the spatial decoupling of the α and ω-effects operation place in the solar convection zone (like in the Babcock-Leighton case), are also known to modulate the long-term variability of the solar cycles (Jouve et al. 2010; Wilmot-Smith et al. 2006), sometimes reaching a chaotic behavior (Charbonneau et al. 2005). In this paper we use a 2D kinematic solar dynamo model merging concepts of the mean-field theory and the Babcock-Leighton mechanism, accounting for different magnetic field strength-limiting thresholds, in order to afford solar-like long-term variability of the solar cycle.

4 Model formulation

To assess the variability of the magnetic field in the kinematic context of the solar dynamo, in which the flow field is steady and prescribed, the problem reduces to solving the MHD induction equation for the magnetic field $\mathbf{B}$

$$\frac{\partial \mathbf{B}}{\partial t} = \nabla \times (\mathbf{U} \times \mathbf{B}) - \nabla \times (\eta_m \nabla \times \mathbf{B}), \tag{1}$$

where $\mathbf{U}$ is the flow field and η_m the magnetic diffusivity. To a first approximation, the large-scale magnetic and flow field can be represented as contributions of their large-scale mean and small-scale fluctuating parts, $\mathbf{B} = \langle \mathbf{B} \rangle + \mathbf{b}'$ and $\mathbf{U} = \langle \mathbf{U} \rangle + \mathbf{u}'$, respectively. Upon substitution of these quantities in equation (1), and proper averaging, we get the mean-field induction equation (Moffat 1978), given by

$$\frac{\partial \langle \mathbf{B} \rangle}{\partial t} = \nabla \times (\langle \mathbf{U} \rangle \times \langle \mathbf{B} \rangle) + \nabla \times (\langle \mathbf{u}' \times \mathbf{b}' \rangle) - \nabla \times \eta_m \nabla \times \langle \mathbf{B} \rangle, \tag{2}$$

The term $\langle \mathbf{u}' \times \mathbf{b}' \rangle$ corresponds to a mean electromotive force $\mathcal{E}$ arising from the interactions of turbulent motions with the small-scaled magnetic field. It can be thus written in terms of a parameterization of the turbulent effects, through the coefficients α and β, on the mean-magnetic field as $\mathcal{E} = \alpha \langle \mathbf{B} \rangle - \beta \nabla \times \langle \mathbf{B} \rangle$. Substitution in the mean-induction equation gives

$$\frac{\partial \mathbf{B}}{\partial t} = \nabla \times (\mathbf{U} \times \mathbf{B}) + \nabla \times (\alpha \mathbf{B}) - \nabla \times \eta \nabla \times \mathbf{B}, \tag{3}$$

for which the brackets indicating averaging have been omitted, but are still considered. The α term represents the magnetic helicity, due to cyclonic motions oriented by the Coriolis force and $\eta = \eta_m + \beta$ is now the effective magnetic diffusivity, covering both magnetic diffusion at the microscopic level and turbulent diffusion, respectively.

An additional important issue arises from working within the kinematic context: How to deal

with the important feedback of the magnetic field modifying fluid motions, via the Lorentz force? Since the motion equation is not solved, this effect ought to be parameterized in the induction equation. This must be done in a way so that the growth of the magnetic field is suppressed above some limiting value, based on the energy equipartion with the turbulent fluid motions. Generally, in the mean-field context, this quenching factor is heuristically formulated as a decreasing function of the magnetic field

$$\alpha(B) = \frac{\alpha_0}{\left(1 + \left(\frac{B}{B_{eq}}\right)^2\right)} \tag{4}$$

B_{eq} being the equipartition magnetic field and α_0 a typical value characterizing the α-effect. Studies of magnetoconvection on the solar interior give $B_{eq} \sim 10^4 G$ (Fan 2009), and led to conjectures that a turbulent α-effect would not represent an effective dynamo mechanism (Cattaneo and Hughes 1996).

Alternatively to the conventional α-effect, Babcock (1961) and Leighton (1969) suggested that the diffusion of the magnetic field of sunspot pairs played a crucial role on the process of poloidal field regeneration. The bipolar sunspot regions are tilted in a way that the magnetic field of the leading spot, nearer the equator, diffuses and reconnects with the field of the leading spot at the other hemisphere - which has nearly always an opposite polarity. At the same time, the magnetic field of the following spot will also decay and connect with the polar magnetic field, which have opposite polarity. This opposite magnetic field from the following spot will at some point annihilate the original polarity of the polar region, causing the magnetic polarity reversion of the initial poloidal field. In this case the poloidal and toroidal fields regeneration processes are spatially segregated, and a means by which the new polar surface magnetic flux generated by the Babcock-Leighton mechanism would be transported to the bottom of the convection zone is necessary. Facing this requirement, initially a meridional circulation flow was assumed in the Babcock-Leighton dynamo modeling. As a matter of fact, a poleward

meridional flow is indeed observed at the solar surface (Duvall 1979). Numerical models comprising on this additional physical ingredient are usually termed flux transport dynamos and they are usually successful in reproducing the equatorward tendency of the toroidal field (Küker et al. 2001). In summary, the meridional flow not only acts as a mean of transporting the polar surface magnetic field down to the base of the convection zone to be transformed into a toroidal field, but drags the toroidal field towards the equator as well, resulting in a solar-like magnetic field behavior.

Simulations of the rising of thin magnetic toroidal flux tubes from the base of the convection zone suggest that for matching the observed tilts, the flux tubes generating sunspots need to have an initial magnetic field strength ranging from approximately 10^4 to 10^5 G. Stronger toroidal flux tubes tend to arise at the solar surface with almost no tilts, while weaker flux tubes arrise at too high latitudes (D'Silva and Choudhurri 1993), hence incompatible with Joy's law. The Babcock-Leighton mechanism would therefore be dependent on the initial intensity of the toroidal flux tube at the base of the convection zone, just above the tachocline.

Despite the observational clues provided by the Babcock-Leighton mechanism, much discussion exists on whether this mechanism is the unique responsible for the poloidal field regeneration, an active but not unique component of this part of the cycle, or yet a mere side effect of the whole process. The first possibility is unlikely, since a dynamo based only on the Babcock-Leighton mechanism is not self-sustainable - it needs the formation of sunspots, and therefore operates only above critical toroidal magnetic field buoyancy values. A probable scenario is that an additional α-effect operates on the convection zone, and the resulting magnetic field is a conjunction of both poloidal field regeneration processes. The three main dynamo processes here discussed, α and ω-effects and the Babcock-Leighton mechanism are schematically shown on Figure 1.

Numerical simulations based on the Babcock-Leighton mechanism have the tendency to produce symmetric solutions relative the equator, opposite to what is observed in the Sun (Chat-

terjee et al. 2004). Recent results have shown that α-effects located within a thin layer just above the tachocline are more successful in giving the right antisymmetric solutions (Bonnano et al. 2008; Dikpati and Gilman 2001). Residual turbulent motions acting on toroidal flux tubes right above the tachocline, before achieving the critical buoyant value, could justify such a disposition of the α-effect. This concept is applied in the present model, in addition to the Babcock-Leighton effect at the solar surface.

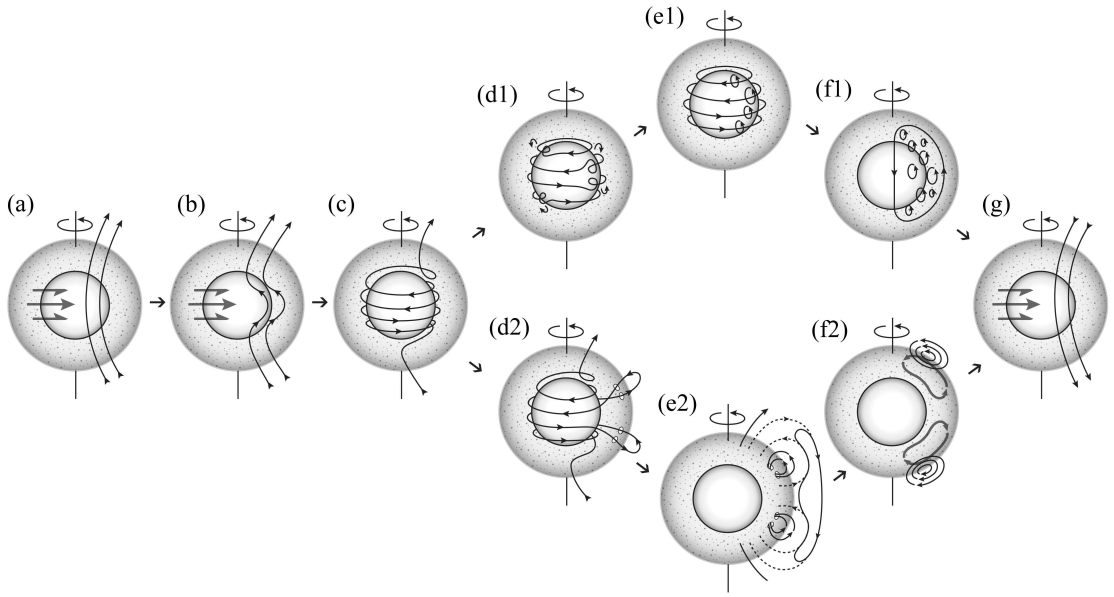

Figure 1: Representative scheme of the main processes thought to occur during the solar cycle, departing from (a), an initial poloidal field. (b) and (c) represent the generation of the toroidal field by differential rotation - the ω-effect. (d1) and (e1) show the effect of cyclonic turbulence on former toroidal fields, creating small-scale secondary poloidal magnetic fields - the α-effect. Averaged, they result in a net electromotive force generating a new large-scale poloidal field (f1), closing the first half part of the cycle with a new poloidal field (g), with opposite polarity than the initial one. (d2) represents the beginning of the Babcock-Leighton mechanism: toroidal fields buoyantly rise to the surface forming sunspots, tilted bipolar regions. In (e2), the field from the bipolar region diffuses and reconnects with the correspondents of each hemisphere and with the polar fields. The resulting poloidal flux is advected by meridional circulation to the poles (f2), generating the final large-scale poloidal field in (g) and transporting the flux to the tachocline.

5 Mathematical description

Under the assumption of axisymmetry, the magnetic and flow fields are written in terms of their poloidal and toroidal components in spherical coordinates (r, θ, t) as

$$\mathbf{B}(r,\theta,t) = \nabla \times (A_\phi(r,\theta,t)\hat{\mathbf{e}}_\phi) + B_\phi(r,\theta,t)\hat{\mathbf{e}}_\phi \tag{5}$$

$$\mathbf{U}(r,\theta) = \mathbf{u_p}(r,\theta) + r\sin\theta\,\Omega(r,\theta)\hat{\mathbf{e}}_\phi \tag{6}$$

in which A_ϕ is the poloidal potential and B_ϕ the toroidal field. The time-independent flow profile is given by the meridional circulation $\mathbf{u}_p$ and the differential rotation Ω. The poloidal-toroidal decomposition of the magnetic field allows a separation of the mean induction equation (3) into two partial differential equations for A_ϕ and B_ϕ

$$\frac{\partial A_\phi}{\partial t} + \frac{Re}{r\sin\theta}\mathbf{u_p}\cdot\nabla\left(r\sin\theta A_\phi\right) = \tilde{\eta}_p\left(\nabla^2 - \frac{1}{r^2\sin\theta^2}\right)A_\phi$$

$$+C_\alpha\alpha(r,\theta;B_\phi)B_\phi + C_S S(r,\theta;B_\phi^{tc})B_\phi^{tc} \tag{7}$$

$$\frac{\partial B_\phi}{\partial t} + Re\; r\;\sin\theta\nabla\cdot\left(\frac{\mathbf{u_p}B_\phi}{r\sin\theta}\right) = \tilde{\eta}_t\left(\nabla^2 - \frac{1}{r^2\;\sin\theta^2}\right)B_\phi$$

$$+\frac{1}{r}\frac{\partial\tilde{\eta}_t}{\partial r}\frac{\partial(rB_\phi)}{\partial r} + C_\Omega\; r\;\sin\theta\,(\nabla\times A_\phi\hat{\mathbf{e}}_\phi)\cdot(\nabla\Omega) \tag{8}$$

The appearance of the terms $C_\Omega = \Omega_{eq}R^2/\eta_S, C_\alpha = \alpha_0 R/\eta_s, C_S = S_o R/\eta_s$ and $Re = u_o R/\eta_s$ results from the nondimensionalization process of the equations using the solar radius R as the characteristic length scale and the effective magnetic diffusion time R^2/η_s as the characteristic time scale. B_ϕ^{tc} is the toroidal field just above the tachocline, and Ω_{eq}, α_o, S_o and u_o are the rotation rate at the equator, typical amplitudes of the poloidal terms and the peak velocity of

the meridional flow at the surface. $\tilde{\eta}_p$ and $\tilde{\eta}_t$ are the normalized effective magnetic diffusivities for the poloidal and toroidal components, respectively. Note that the extra α-term that would arise in equation (8) has been neglected, as it is common in the solar case approximation to suppose that $C_\Omega >> C_\alpha$. The flow specifications, $\mathbf{u}_p$ and Ω are the same as the ones used in the reference work of Dikpati and Charbonneau (1999), and are shown in the left panels of Figure 2. The tachocline depth and thickness is still uncertain. In this paper, the tachocline will comprise the region from the top of the radiative zone, $r_b = 0.6R$, to the top of the region with the largest radial angular velocity gradient, $r_t = 0.7R$.

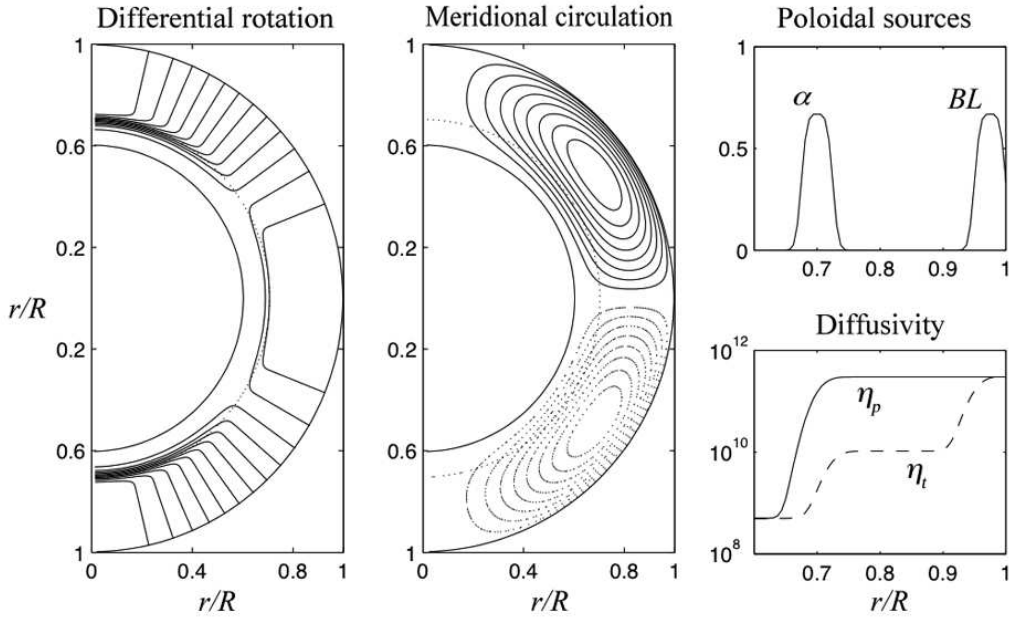

Figure 2: Specifications of the model. Left: isocontours of $\Omega(r, \theta)$ based on analytic fit of the differential rotation profile from helioseismology data. Center: meridional circulation streamlines (full line - counterclockwise flow, dotted line - clockwise flow). Right top: poloidal source profiles. Right bottom: effective magnetic diffusivity profiles.

It is worth noticing that the S term, representing the Babcock-Leighton poloidal regeneration process at the surface, has been added in an ad-hoc manner to equation (7). Differently from the α-term, it is non-local - it depends on the toroidal field at the tachocline. This comes from the latitudinal tilt given by Joy's law being rather dependent on the initial magnetic field

strength of the rising flux tube, therefore at the tachocline (D'Silva and Choudhurri 1993). The α-effect on equation (7) must be suppressed for magnetic field strength above a limiting value associated with energy equipartition. Therefore, the α-term will be written evoking expression (4), as

$$\alpha(r,\theta;B_\phi) = \frac{1}{\left(1+\left(\frac{B_\phi}{B_{eq}}\right)^2\right)} f_\alpha(r,\theta) \tag{9}$$

where $B_{eq} = 10^4$ G and $f_\alpha(r,\theta)$ is a function of spatial coordinates given by

$$f_\alpha(r,\theta) = \frac{1}{4}\left[1+erf\left(\frac{r-r_1}{d_1}\right)\right]\left[1-erf\left(\frac{r-r_2}{d_2}\right)\right]\cos\theta\sin\theta \tag{10}$$

where $r_1 = 0.675R$, $r_2 = 0.725R$ and $d_1 = d_2 = 0.01R$. This function constrains the α-effect to a thin layer at the base of the convection zone, just above the tachocline, and to midlatitudes. Similar conjectures apply for the Babcock-Leighton S source term on equation (7), with the difference that it works within lower and upper limiting values

$$S(r,\theta;B_{\phi\,tc}) = \frac{1}{4}\left[1+erf\left(B^2_{\phi\,tc}-B^2_{\phi\,tc\,min}\right)\right]\left[1-erf\left(B^2_{\phi\,tc}-B^2_{\phi\,tc\,max}\right)\right] f_S(r,\theta) \tag{11}$$

Here $B_{\phi\,tc\,min} = 10^4$ G, $B_{\phi\,tc\,max} = 10^5$ G and the radial and latitudinal distribution $f_S(r,\theta)$ is given by

$$f_S(r,\theta) = \frac{1}{4}\left[1+erf\left(\frac{r-r_3}{d_3}\right)\right]\left[1+erf\left(\frac{r-r_4}{d_4}\right)\right]\cos\theta\sin\theta \tag{12}$$

where $r_3 = 0.95R$, $r_4 = 1.0R$ and $d_3 = d_4 = 0.01R$, restricting the Babcock-Leighton mechanism to the near-surface layers. The poloidal source terms α and S profiles with respect

to the radial distribution are shown in the right panel of Figure 2.

The effective diffusivities are given following the concept from Chatterjee et al. (2004), in which they parameterize the effect of turbulent diffusion suppression by separating the diffusivity into poloidal η_p and toroidal η_t components.

$$\eta_p = \eta_c + \eta_s \, \frac{1}{2}\left[1 + erf\left(\frac{r - r_5}{d_5}\right)\right] \tag{13}$$

$$\eta_t = \eta_c + \eta_{cz} \, \frac{1}{2}\left[1 + erf\left(\frac{r - r_6}{d_6}\right)\right] + \eta_S \, \frac{1}{2}\left[1 + erf\left(\frac{r - r_7}{d_7}\right)\right] \tag{14}$$

in which $r_5 = 0.7R$, $r_6 = 0.72R$, $r_7 = 0.95R$ and $d_5 = d_6 = d_7 = 0.025R$. Such separation comes from the fact that the toroidal field, at least in deeper layers, tend to be much more intense than the poloidal field, and therefore more effective in suppressing the turbulent diffusion effects. η_c is the core diffusivity near the radiative zone, η_{cz} the diffusivity in the turbulent convection zone associated with the toroidal magnetic field, and η_S the diffusivity in the radial surface layers and for the weaker poloidal field. They are set in this study to $\eta_c = 5 \times 10^8$ cm^2/s, $\eta_{cz} = 1 \times 10^{10}$ cm^2/s and $\eta_s = 3 \times 10^{11}$ cm^2/s. The radial profiles are shown in the right panel of Figure 2.

6 Numerical simulation

Given the described physical ingredients, equations (7) and (8) are solved numerically over a regular grid in an annular meridional plane covering $\theta \in [0, \pi]$ and $r \in [0.6, 1]$, that is, from slightly below the tachocline up to the solar surface. The boundary and initial condition specifications used are the following: the inner boundary condition is set as to represent the radiative zone as a perfect conductor. An approximation of this condition gives that at $r = 0.6$, $A_\phi = B_\phi = 0$ (Chatterjee et al. 2004). The outer boundary condition is for a vacuum region, requesting a smooth match with a potential magnetic field (Dikpati and Charbonneau 1999). As for the initial condition, a dipolar field confined to the convective envelope is used. In this case, $A_\phi = \sin\theta/r^2$ for $r \geq 0.7R$ and zero for all other r, whereas $B_\phi = 0$ for all r.

The solution procedure was performed by an adaptation of the Parody code (Dormy et al. 1998), based on a semi-spectral method. It consists in spherical harmonic expansion for the angular components of the poloidal and toroidal scalars and finite differences in the radial direction over a full spherical shell. More details on the code are presented in the Appendix. The results here presented were performed with maximum harmonic degree $L_{max} = 65$, number of radial points $N_r = 65$ and a constant time stepping of $\Delta t = 5 \times 10^{-6}$.

7 Results

On the basis of helioseismic data ($\Omega_{eq} = 2\pi \times 460.7$ nHz), we fix $C_\Omega = 4.7 \times 10^4$; for this case, variations of the free parameters C_α, C_S and Re allow for a broad range of solutions. Meridional circulation measured at the solar surface at mid-latitudes displays an average value of 15 m/s. Considering Re varying around this value, from 318 to 378, the minimum configuration for a proper dynamo solution consists in approximately $C_\alpha = 2$ and $C_S = 0.5$. In order to access the solar representativeness of the solution, some observable aspects should be matched (Charbonneau 2010):

1. Cyclic polarity reversals with approximately 11 years periodicity;
2. Strong deep toroidal fields ($\sim 10^4 - 10^5 G$) at a 30^o latitudinal belt migrating equatorward;
3. Poleward migration of the polar radial field ($\sim 10 - 100G$);
4. Phase lag of $\pi/2$ between the deep mid-latitudinal toroidal and surface polar fields;
5. Antisymmetric coupling of the magnetic fields between the hemispheres;
6. Long-term variability of the solar cycle.

A useful way to analyze the solar semblance of the model results is to display the magnetic field in a time-latitude map and compare it with proper synoptic magnetograms and sunspot butterfly diagrams (Hathaway 2010). A reference solution of the model is displayed in this form in Figure 3, in which the surface polar field contours are superimposed with the grey-scale map of the toroidal field just above the tachocline ($r_{tc} = 0.7R$). This case was chosen for matching most of the observed requisites. Criterion 1, for example: the periodicity associated with the solar cycle is of 10.95 years. The main dependence of the periodicity resides on the strength of meridional circulation, a well-known characteristic of flux transport dynamos (Dikpati and Charbonneau 1999). Using a similar model as the present one, Charbonneau et al. (2005) observed the persistent dominance of the meridional circulation on setting the cycle

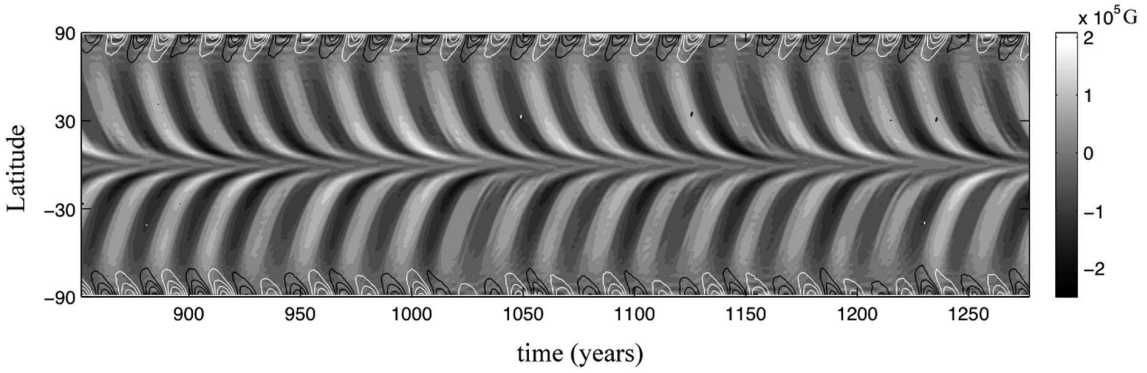

Figure 3: Butterfly diagram of the dynamo solution corresponding to $C_S = 1.0$, $C_\alpha = 8.0$ and $Re = 318$. The grey-scale map represents the toroidal field at the tachocline, whereas high latitude black and white contours represent the radial field at the solar surface, with a maximum value of 1700 G.

periodicity even in a chaotic regime of the dynamo, in which the present solutions were found. The morphology presented in criteria 2 and 3 was also achieved, even though the polar strength of most of the solutions (peaking 1700 G for the cited case) is an order of magnitude higher than the observed. A phase lag of approximately $\pi/2$ between poloidal and toroidal fields cited in criterion 4 is also a general property of flux transport Babcock-Leighton models (Dikpati and Charbonneau 1999).

On the other hand, the parity requisition 5 is still an issue. Although the inclusion of an α-effect at a thin layer above the tachocline was thought to help yielding anti-symmetric solutions (Bonnano et al. 2008; Dikpati and Gilman 2001), the parity coupling was not straightforward in this model case. Actually, it does not seem to exist a clear preferred mode for the solutions: they vary between periods of symmetric, anti-symmetric and out of phase modes. In the reference case, as it is noticeable in Figure 3, the activity in both hemispheres was slightly out of phase. This probably originates from the chaotic nature of the solutions. For higher dynamo numbers, C_S and C_α, there was a tendency for the magnetic fields to evolve independently in each hemisphere - with no fixed phase relation. Charbonneau et al. (2005) analyzed the general chaotic behavior in a Babcock-Leighton dynamo and concluded it is caused by time-delays

occuring from the spatial decoupling of the toroidal and poloidal field regeneration processes. Long-term variability commented on item 6 is a clear consequence of such time-delays. Figure 4 displays the evolution of the toroidal magnetic field energy at a certain latitude - toroidal magnetic field energy is generally used as a proxy for activity cycle amplitude. The chaotic evolution of the solution is evident, displaying long-term modulations of the solar cycle. In addition, there are also periods of grand minima, in which the cycle is apparently not fully developed, but persist with a kind of residual activity.

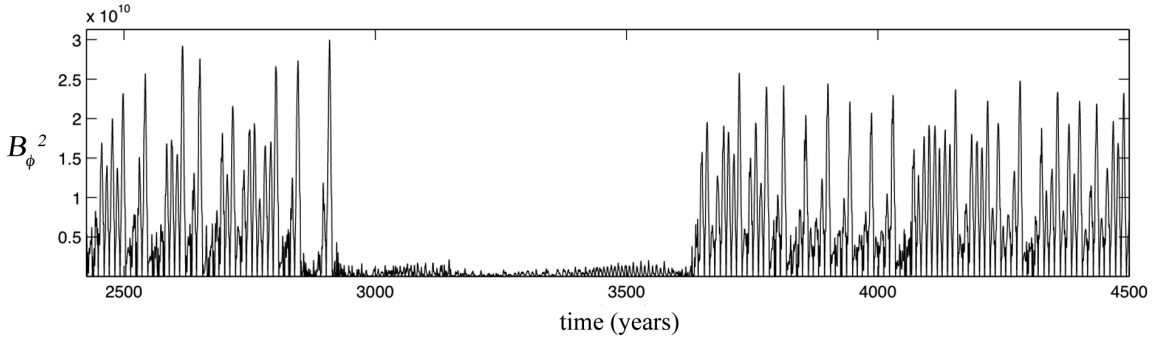

Figure 4: Time series of the toroidal magnetic energy at the tachocline at 20^o latitude for the reference solution. Apart from the clear modulation of the solar cycle there is also the presence of an extended period of minimum activity, where supposedly the toroidal magnetic field do not achieve the critical value for buoyant instability, leading to sunspot forming.

The residual activity episode shown in Figure 4 suggests there are two different regimes for the solar large-scale magnetic field behavior. Considering we have at hand two different mechanisms for the poloidal field regeneration process, this could indicate the predominance of one relative to the other. Motivated by this thought, we show in Figure 5 the toroidal magnetic energy time series of two models, one with only the α-effect at the tachocline and the other considering only the Babcock-Leighton regeneration process at the solar surface. In the Babcock-Leighton case, the solar cycle evolution is smooth and tends to display a persistent weak-strong amplitude bundling configuration (therefore with twice the cycle period). This resembles the observed solar pattern known as the Gnevyshev-Ohl rule, also a consequence of the time-delays inherited by the Babcock-Leighton mechanism (Charbonneau et al. 2007).

The situation is different in the α-effect poloidal source case in which the general amplitudes of the cycles are much lower, the cycle period is about twice as long, and there are additional high frequency oscillations over the solar cycles.

Aware of the different behaviors concerning the different poloidal field regeneration processes, it is possible that the period of minimum activity involves the preponderance of the tachocline α-effect over the Babcock-Leighton mechanism. In such case, lower initial poloidal fields would result in the generation of toroidal field below the buoyancy instability limit, leading to few sunspot formations. The long term solar cycle variability would then mainly be driven by the tachocline α-effect, generating weak toroidal fields during periods of minimum activity, but being able to restart the Babcock-Leighton mechanism when the upper threshold of toroidal field strength is achieved. This situation matches the observable minimum activity periods, like the Maunder Minimum.

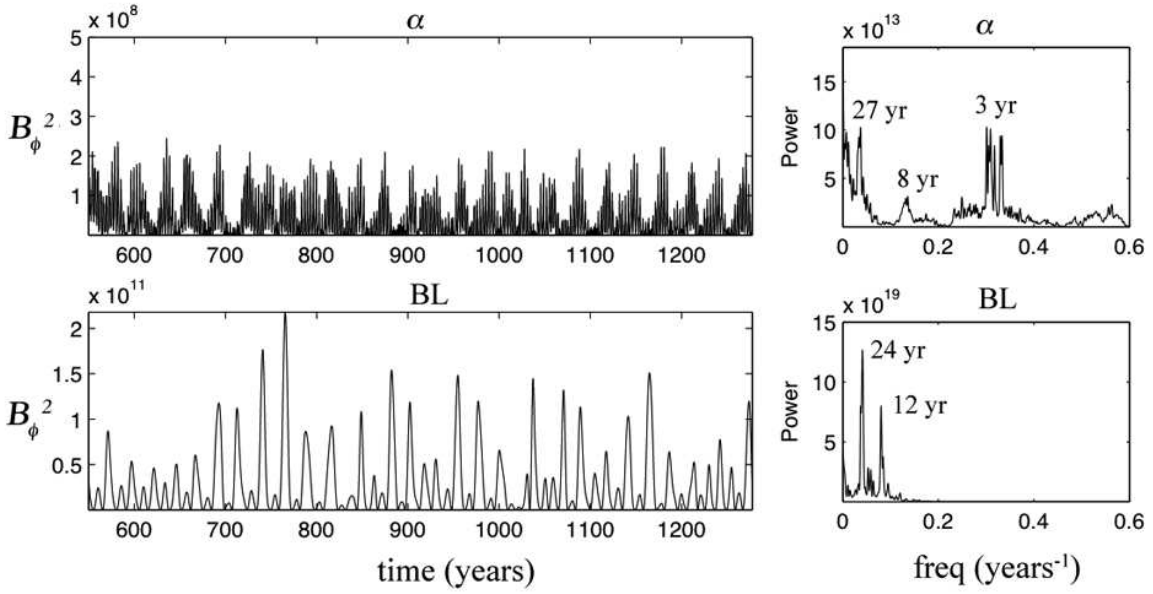

Figure 5: Toroidal magnetic energy at the tachocline at 20^o latitude and the respective power spectra of two different dynamo models: with only α-effect, $C_\alpha = 8.0$, at the tacholcline (upper panel) and another with only Babcock-Leighton poloidal source, $C_s = 4.0$, at the surface (lower panel). For both cases $Re = 378$.

8 Conclusion

In view of the not self-sustainable character of a solar dynamo relying only on the Babcock-Leighton mechanism for poloidal field regeneration, we have considered an additional α-effect operating in a thin layer above the tachocline, originating from the turbulent effects on magnetic flux tubes just above the critical buoyancy level. Accounting for different limiting ranges of magnetic field intensity on the operation of each effect (concerning their different natures) we have managed to obtain a dynamo solution with the basic solar magnetic field dynamic features, to list: cyclic reversions with a ~ 11 year periodicity, equatorward migration of the activity belt, poleward migration of the polar radial field, proper phase lag between both and long-term variability resembling the solar activity variations.

Antisymmetric coupling of the magnetic field between the hemispheres is still an issue, despite the α-effect at the tachocline being suggested as a way to circumvent the parity problem. In fact, the hemispheres appear to behave in a rather dissociated way, showing no preferred relaxation mode. The main reason for the decoupling may come from the chaotic nature of the solution, making the magnetic field of each hemisphere to evolve independently. Further investigations on the parity topic are needed, possibly relying in a harmonic analysis of the variability of the magnetic fields in each hemisphere and comparison with harmonic decompositions of the solar surface magnetic field, as in Stenflo and Vogel (1986).

We conclude by suggesting that the grand minima periods characterizing suppressed magnetic activity could be caused by an intermittent state in the solar dynamo, such that only a deep and weak α-effect is responsible for the poloidal field regeneration. It thus raises a question on what would be the reason for the dominance of the α-effect regime over the Babcock-Leighton mechanism in regenerating the poloidal field.

9 Acknowledgements

We would like to thank Dr. Oscar Matsuura for the valuable suggestions and discussions. This work is a result of a M.Sc. project in collaboration between Observatório Nacional and IPGP. We thank both institutions for the available facilities and the Brazilian agency CAPES for funding this research.

10 Appendix

Parody Code - Mean Field Benchmarking

The Parody code used in this work was originally proposed for full 3D MHD dynamo simulations (ACD code, benchmarked in Christensen et al. 2001). The magnetic field is decomposed in the form

$$\mathbf{B} = \nabla \times \nabla \times (B_p\, \mathbf{r}) + \nabla \times (B_t\, \mathbf{r})\,, \tag{15}$$

and the scalar potentials further expanded in a spherical harmonics basis, writing

$$B_{p,t} = \sum_{\ell=1}^{L_{max}} \sum_{m=0}^{M_{max}} B_{p,t}(r,t)_\ell^m\, Y(\theta,\phi)_\ell^m. \tag{16}$$

The radial dependence is treated by a second-order finite-differencing scheme. Time integration uses a Crank-Nicholson scheme for diffusion terms and an Adams-Bashforth scheme for the nonlinear terms. The actual equations to be solved are the radial curl and radial curl of the curled induction equation (1). Further adaptation to the axisymmetric ($M_{max} = 0$) mean-field scenario considered: changing of the inner boundary condition, flow specification by differential rotation and meridional circulation, construction of the proper diffusivity profiles and inclusion of the α and S terms in the induction equation. The original inner boundary conditions consisted on insulating or electric conductor cases, and the changes considered the perfect conductor case. Such modification consisted in writing $B_p = 0$ and $\partial(rB_t)/\partial r$ at the inner boundary.

Upon the adaptations, the code was tested by comparing the results with the reference solutions of a mean-field solar dynamo benchmark from Jouve et al. (2008). Such benchmarking consisted in accessing the critical dynamo numbers of two cases considering an $\alpha\omega$ mean-field dynamo (cases A and B, differing only in the different treating of the diffusivity) and one based on the Babcock-Leighton mechanism (case C), as well as their cycle frequency, and comparing

them with other code's results relying on different numerical methods. Table 1 displays the values obtained from Parody's adaptation and the reference ones for the cases treated in Jouve et al. (2008), evidencing a proper matching. The butterfly diagrams for the supercritical cases (SB and SC), which considers the α-quenching, are displayed in Figure 6.

Table 1: Comparison of the critical dynamo numbers and frequency of the solar cycle with the benchmark cases A, B and C.

	Results			Reference	
Case	Resolution	C_α^{crit}	ω	C_α^{crit}	ω
A	71×71	0.385	158	0.387 ± 0.002	158.1 ± 1.472
B	71×71	0.406	172	0.408 ± 0.003	172.0 ± 0.632
C	120×120	2.546	534	2.489 ± 0.075	536.6 ± 8.295

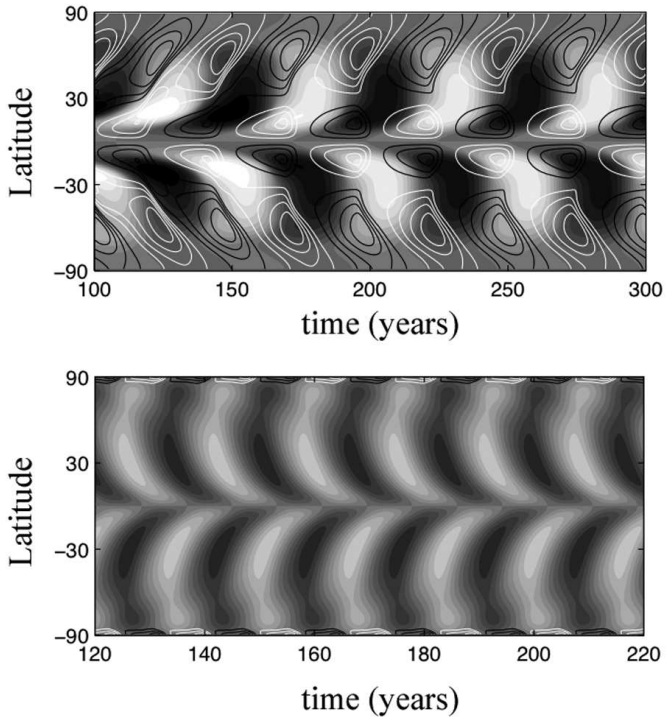

Figure 6: Butterfly diagram summarizing the Benchmark cases. Contours refer to the radial field at the surface an grey-scale map to the toroidal field at the tachocline. Upper panel: $\alpha\omega$ dynamo with from case SB. Lower panel: Babcock-Leighton dynamo from case SC.

11 References

BABCOCK H W. 1961. The Topology of the Sun's Magnetic field and the 22-Year Cycle. Astrophys J 133: 572-589.

BAKER D. 2000. The occurrence of operational anomalies in spacecraft and their relationship to space weather. IEEE T Plasma Sci 28: 2007-2016.

BEER J, TOBIAS S AND WEISS N. 1998. An active sun thoughout the Maunder Minimum. Sol Phys 181: 237-249.

BONNANO A, ELSTNER D, RUDIGER G AND BELVEDERE G. 2008. Parity properties of an advection-dominated solar α^2 Ω-dynamo. Astron Astrophys 390: 673-680.

BUSHBY PJ. 2006. Zonal flows and grand minima in a solar dynamo model. Monthly Notices of the Royal Astronomical Society 371: 772-780.

CATTANEO F AND HUGHES D. 1996. Nonlinear saturation of the turbulent α effect. Astrophys J Lett 515: L39-L42.

CHARBONNEAU P. 2010. Dynamo models of the Solar Cycle. Living Reviews in Solar Physics 7, http://www.livingreviews.org/lrsp-2010-3.

CHARBONNEAU P, BEAUBIEN G, ST-JEAN C. 2007. Fluctuations in Babcock-Leighton dynamos. II. Revisiting the Gnevyshev-Ohl rule. Astrophys J 658: 657-662.

CHARBONNEAU P, ST-JEAN C AND ZACHARIAS P. 2005. Fluctuations in Babcock-Leighton dynamos. I. Period doubling and transition to chaos. Astrophys J 619: 613-622.

CHARBONNEAU P, BLAIS-LAURIER G AND ST-JEAN C. 2004. Intermitency and phase persistence in a Babcock-Leighton model of the solar cycle. Astrophys J 616: L183-L-186.

CHARBONNEAU P. AND DIKPATI M. 2000. Stochastic fluctuations in a Babcock-Leighton model of the solar cycle. Astrophys J 543: 1027-1043.

CHATTERJEE P, NANDY D AND CHOUDHURI AR. 2004. Full-sphere simulations of a circulation-dominated solar dynamo: Exploring the parity issue. Astron Astrophys 407: 1019-1030.

CHOUDHURI AR. 1992. Stochastic fluctuations of the solar dynamo. Astron Astrophys 253: 277-285.

CHRISTENSEN UR, et al. 2001. A numerical dynamo benchmark. Phys Earth Planet In 128: 25-34.

DIKPATI M AND GILMAN D. 2001. Flux-transport dynamos with α-effect from global instability of tachocline differential rotation: a solution for magnetic parity selection in the sun. Astrophys J 559: 428-442.

DIKPATI M, CHARBONNEAU P. 1999. A Babcock-Leighton flux transport dynamo with solar-like differential rotation. Astron J 518: 508-520.

DORMY E, CARDIN P, JAULT D. 1998. MHD flow in a slightly differentially rotating spherical shell, with conducting inner core, in a dipolar magnetic field. Earth Planet Sc Lett 160: 15-30.

D'SILVA S AND CHOUDHURI AR. 1993. A theoretical model for tilts of bipolar magnetic regions. Astron Astrophys 272: 621-633.

DUVALL JR TL. 1979. Large-scale solar velocity fields. Sol Phys 63: 3-15.

FAN Y. 2009. Magnetic fields in the solar convection zone. Living reviews on Solar Physics, 6: http://www.livingreviews.org/lrsp- 2009-4.

HAIGH J. 2003. The effects of solar variability on the Earth's climate. Philos T Roy Soc Lond 361: 95-111.

HATHAWAY DH. 2010. The solar cycle. Living Reviews in Solar Physics 7, http://www.livingreviews.org/lrsp- 2010-1.

HOWE R, CHRISTENSEN-DALSGAARD J, HILL F, KOMM RW, LARSEN RM, SCHOU J, THOMPSON MJ AND TOOMRE J. 2000a. Dynamic Variations at the base of the

Solar Convection zone. Science 287: 2456-2460.

JOUVE L, PROCTOR MRE, LESUR G. 2010. Buoyancy-induced time delays in Babcock-Leighton flux-transport dynamo models. Astron Astrophys 517:?

JOUVE L, BRUN AS, et al. 2008. A solar mean field dynamo benchmark. Astron Astrophys 483: 949-960.

KÜKER M, RUDIGER G, SCHULTZ M. 2001. Circulation-dominated solar shell dynamo models with positive alpha-effect. Astron Astrophys 374: 301-308.

LEIGHTON R. 1969. A magneto-kinematic model of the solar cycle. Astrophys J 156: 1-26.

MAKAROV VI, TLATOV AG, CALLEBAUT DK, OBRIDKO VN and SHELTING BD. 2000. Large-scale magnetic field and sunspot cycles. Sol Phys 198: 409-421.

MOFFAT HK. 1978. Magnetic field generation on electrically conducting fluids. Cambridge University Press. Cambridge.

OSSENDRIJVER M. 2003. The solar dynamo. Astron Astrophys Rev 11: 287-367.

PARKER EN. 1979. Sunspots and the physics of magnetic flux tubes. I. The general nature of the sunspot. Astrophys J 230: 905-913.

PARKER EN. 1955. Hydromagnetic dynamo models. Astrophys J 122: 293-314.

SOLANKI SK. 2003. Sunspots: An Overview. The Astron Astrophys Rev 11: 153-286.

SCHOU J ET AL.1998. Helioseismic studies of differential rotation in the solar envelope by the solar oscillations investigation using the Michelson Doppler Imager. Astrophys J 505: 390-417.

WILMOTH-SMITH AL, NANDY D, HORNIG G AND MARTENS PCH. 2006. A time delay model for solar and stellar dynamos. Astrophys J 652: 696-708.